Ethylene Glycol-water Based Graphene Oxide Nanofluid as Corrosion Inhibitor in Automotive Radiator

I.Habibi [1], Saifudin [1], H. R.Fatoni [1], R. Kusumastuti [2], G.Priyotomo [2], S.Musabikha [2], A.Nikitasari [2], S.Prifiharni [2], Y. Lestari[2], A.Royani[2]

[1] Department of Mechanical Engineering, Universitas Muhammadiyah Magelang
Jl. Mayjend Bambang Soegeng KM 5 Mertoyudan , Magelang, Jawa Tengah, Indonesia

[2] Research Center for Metallurgy, BRIN
Gd.720. KST B.J.Habibie, Puspiptek Area, Serpong, Tangerang Selatan, Banten, Indinesia

Email: raha006@brin.go.id; habibi@unimma.ac.id

Abstract
A rapid cooling process is essential to maintain an optimal working temperature in a vehicle, which directly impacts its efficiency. Corrosion is a persistent and inevitable damage in cooling systems that use water-based fluids. The current challenge is to explore water-based fluids that not only exhibit excellent corrosion resistance but also possess superior heat conduction properties to improve vehicle efficiency. This study investigated the incorporation of Graphene Oxide, renowned for its corrosion inhibition properties, into ethylene glycol/water solution to assess its protective efficacy on Al6061 material. A series of analytical methods, including Optical Emission Spectroscopy (OES), pH, conductivity, Fourier-Transform Infrared Spectroscopy (FTIR), and polarization techniques, are used to evaluate the corrosion inhibition performance of graphene oxide at various concentrations and under different ambient temperatures. The results showed a decrease in pH value and conductivity with increasing concentration of graphene oxide. FTIR analysis confirmed the formation of a protective layer on the surface of Al6061. Corrosion rate assessment was performed on Al6061 samples immersed in ethylene glycol/water mixture with graphene oxide concentrations of 0, 0.03%, 0.05%, and 0.10%. There was a significant decrease in corrosion rate with the addition of graphene oxide to the cooling system: at 30 ° C, the rate decreased to 4.620, 3.308, 2.565, and 1.006 mpy; at 40°C, up to 4,728, 2,541, 1,503, and 1,270 mpy; and at 50°C, up to 5.629, 1.146, 2.947, and 1.441 mpy, corresponding graphene oxide concentrations of 0.03%, 0.05%, and 0.1%, respectively. Experimental data confirmed that graphene oxide effectively reduces the corrosion rate of Al6061 in ethylene glycol/water mixtures. The study concluded that the use of graphene oxide as a corrosion inhibitor markedly improved the resistance and performance of Al6061 in ethylene glycol/water, with graphene oxide contributing to this protective mechanism through the process of physisorption.

Keywords: Ethylene Glycol, Graphene oxide, Cooling systems, Al 6061, Corrosion Inhibitor

1. Introduction

With the progression of technological advancements, engine cooling has emerged as a complex technical challenge across various industrial sectors, such as automotive, electrical, and manufacturing. The cooling system is crucial for the engine's proper functioning, utilizing various media like water, engine oil, mineral oil, and ethylene glycol (EG) for diverse applications [1]. While these systems offer benefits, they also face efficiency drawbacks, especially in terms of heat transfer and thermal conductivity[2]. Such inefficiencies can lead to increased fuel consumption, reduced engine efficiency, heightened fuel evaporation, elevated pollution levels, and potential damage to engine components that may be difficult or impossible to repair[3-4]. Consequently, researchers and industrial practitioners are exploring innovative solutions to enhance engines' heat transfer and cooling efficiency[5]. These efforts aim to improve engine performance, reduce fuel consumption, lower pollution levels, extend engine component lifespan, and enhance the cooling system's overall reliability [6]. The advent of nanofluid technology presents novel approaches to improving heat transfer rates [7-8]. Introducing nanoparticles

into coolant systems has broadened research avenues, exploiting the higher thermal conductivity of solid particles over liquids [9]. Nanofluids, comprising solid nanoparticles (<100 nm) like metal oxide and metal particles suspended in a fluid, have demonstrated potential in increasing cooling system efficiency [10]. Notably, Peyghambarzadeh et al.'s investigation into the Al2O3/Ethylene Glycol-Water nanofluid as a radiator coolant showed a 40% improvement in heat transfer compared to the base fluid. This study, along with similar research by Zakaria et al., which reported an 8.5% increase in thermal conductivity with the addition of 20 nm-sized Al2O3 nanoparticles at a 0.8% volume fraction in water and ethylene glycol, highlights the significant potential of nanofluids in enhancing cooling system efficiency [11]. These enhancements are attributed to the suspended nanoparticles, which increase surface area and heat capacity, significantly boosting the coolant fluid's thermal conductivity [12]. Corrosion within cooling systems presents a significant issue, impairing optimal engine function [13]. This challenge is especially prevalent in systems using water-based fluids [14]. Corrosion inhibitors have been developed for water-based fluids, as corrosion can lead to leaks and system failure, potentially resulting in engine damage due to overheating [15-16]. The exploration of corrosion in automotive cooling systems, a relatively under-investigated area, the need for developing water-based coolant fluids that can efficiently conduct heat while preventing corrosion [17-18],[13]. Graphene oxide (GO), known for its corrosion inhibition properties under harsh conditions, has begun to be incorporated into nanofluids for cooling systems [19-21]. Studies, including those by Ijaz et al and Shankara et al., have demonstrated significant increases in cooling efficiency and heat transfer with the addition of GO nanoparticles to coolant fluids[22]. This research emphasizes the importance of investigating the corrosion rate of radiator materials under graphene oxide protection within cooling systems [23]. Thus, this study seeks to assess the impact of graphene oxide protection on the corrosion rate of Al 6061 material, used as radiator material, in an ethylene glycol-water-based cooling fluid.

2. Methods

This research is a collaboration between the Department of Mechanical Engineering, University of Muhammadiyah Magelang (Unimma), and the Metallurgical Research Center of the National Research and Innovation Agency (BRIN). The research was conducted in two different laboratories: the automotive laboratory at Unimma and the corrosion laboratory at the Metallurgical Research Center, BRIN. The following are the stages of the research method, likely:

2.1. Materials preparation

a. Optical Emission Spectroscopy (OES) Measurement

Optical Emission Spectroscopy (OES), is a rapid method for determining the elemental composition of a variety of materials. The material radiator is prepared for corrosion testing, Al 6061 specimens were prepared for corrosion testing, and the chemical composition of AA6061 is shown in Table 1. The dimensions of the specimens were shaped like a coin with a diameter of 12 mm and a thickness of 3 mm as shown in ***Figure 1.*** The surface of the specimen was finished using sandpaper sequentially from grade 400-1500, then polished using autosol. Mechanical properties of the ASTM A36 Steel and Experimental results comparison, are shown in Table 2.

Table 1. Chemical composition of Al6061

Elements	Si	Fe	Cu	Mn	Mg	Cr	Zn	Ti	Al	Elements
AA6061 (% wt)	0.581	1,484	0,159	0,163	> 0,240	0.620	0,0049	0,183	>10,80	AA6061 (% wt)

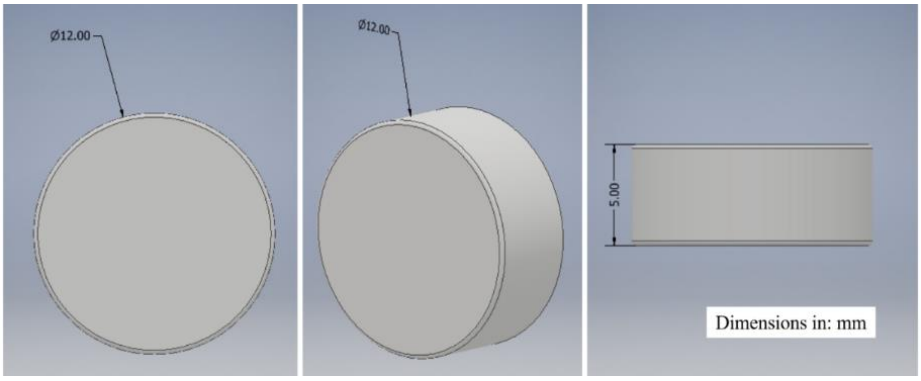

Figure 1. Dimensions of corrosion test specimens (dimensions in mm)

Table 2. Mechanical properties of the ASTM A36 Steel and Experimental results comparison.

Mechanical properties	ASTM specification	Experimental result
Ultimate tensile strength (MPa)	400-450	400-560
Yield tensile strength (MPa)	250	300
Elongation at break (%, 50 mm)	23	10-14
Hardness Vickers Number (HVN)	168.99	276.2
Mechanical properties	ASTM specification	Experimental result

b. Preparation of Nanofluids

Graphene oxide (GO) nanoparticles with an average diameter of 2 nm and used to prepare the nanofluid. Nanofluids were prepared with a mixture composition of 75% water, 15% ethylene glycol and 10% nitrite. GO nanoparticles were added to the cooling water mixture with variations of 0.03%, 0.05%, and 0.1% wt. % addition. A 22 kHz setting was used on an ultrasonic device during the preparation which was done for 4 hours.

c.pH measurements

The pH measurement was conducted using a Hanna HI 98107 pH meter.

d.Thermal conductivity measurements

The conductivity measurement was conducted using a HANNA HI 98192 conductivity meter.

e.Infrared Measurements

FTIR analysis is used for compound functional group analysis using the Fourier Transform Infrared (FTIR) tool Shimadzu Brand, Type: IRPrestige21

f. Electrochemical Measurement

The electrochemical investigation was conducted using Gamry's polarization equipment, which employed three electrodes. The reference electrode utilized was a saturated calomel electrode (SCE),

the counter electrode was made of platinum, and the working electrode consisted of Al6061 material. The potentiodynamic polarization test was executed over a potential range of +250 mV to -250 mV, both in the absence and presence of a graphene oxide inhibitor, at a scan rate of 1 mV/s. An analysis of the corrosion rate was performed to assess the impact of incorporating Graphene Oxide into the cooling nanofluid mixture (ethylene glycol + water) on the Al6061 material, which serves as the radiator material. Corrosion rate analysis was carried out with 3 variant concentrations of graphene oxide nanoparticles: 0.03%, 0.05%, and 0.1% wt. Corrosion rate analysis was carried out with a Gamry-600 potentiostat at the corrosion laboratory, metallurgy research center, BRIN KST BJ. Habibie, Serpong. South Tangerang.

3. Results and Discussion

The research involved several key procedures: analyzing the pH and conductivity of the solution, performing Fourier Transform Infrared (FTIR) spectroscopy, and evaluating the corrosion rate of Al 6061 material in ethylene glycol water-based solutions with varying concentrations and temperatures of Graphene Oxide (GO). The concentrations of GO examined were 0.03%, 0.05%, and 0.10%, while the temperature conditions tested were 30°C, 40°C, and 50°C.

a. pH Measurement

The results of the pH analysis of the solution as shown in Figure 2.

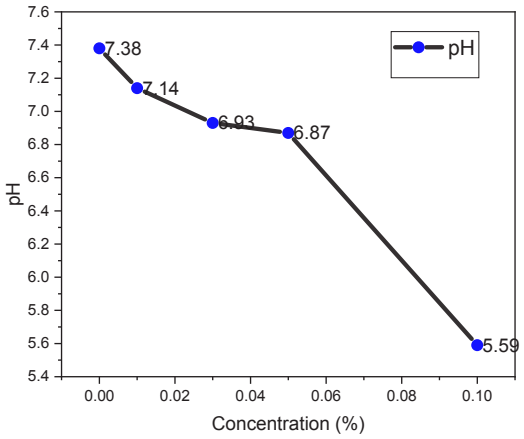

Figure. 2. The graphene oxide concentration in ethylene glycol/water vs. the pH

The results of the pH analysis of the solution as shown in Figure 2. Interactions of graphene oxide (GO) particles with the solution: increasing the concentration of graphene oxide (GO) leads to a higher number of graphene oxide (GO) particles in the ethylene glycol/water. Graphene oxide (GO)particles can interact with water and ethylene glycol molecules in the solution. These interactions can cause changes in the acidity or alkalinity of the solution, which are reflected in changes in the pH value. Ionization reaction of graphene oxide (GO): At certain concentration levels, graphene oxide (GO) particles can undergo ionization reactions in the solution. This ionization reaction can produce hydrogen ions (H^+) or hydroxide ions (OH^-) in the solution, which affects the overall pH of the solution. Effect of carbonyl on graphene oxide (GO): The presence of carbonyl groups in the graphene oxide (GO) structure can enhance its reactivity with water and ethylene glycol. The reaction between carbonyl groups and water or ethylene glycol can produce compounds with acidic properties, which can lower the pH of the solution. Furthermore, further depth research

is needed to understand the mechanisms of pH changes and ensure that the pH decrease does not have any negative effects on the cooling system and the materials involved.

b. Conductivity Measurement

The effect of graphene oxide variations in concentration in ethylene glycol/water on the conductivity of the solution is shown in Figure 3.

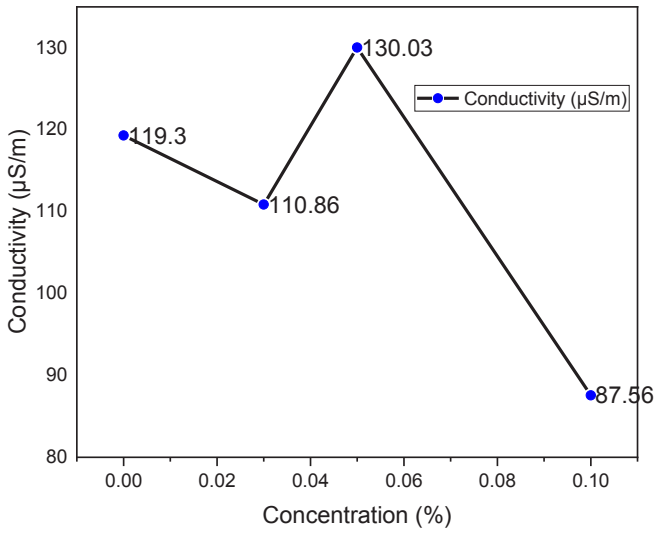

Figure 3. The graphene oxide concentration in ethylene glycol/water vs. the conductivity

The effect of graphene oxide variations in concentration in ethylene glycol/water on the conductivity of the solution is shown in Figure 3. The increase of graphene oxide concentration in EG/water solution causes a tendency to decrease in conductivity. This occurs due to the interaction between graphene oxide (GO) particles and water/ethylene glycol molecules, through van der Waals bonds and electrostatic forces. The interaction between graphene oxide (GO) particles and ethylene glycol/water molecules can hinder the flow of electric charge (electrons) in the solution. Graphene oxide (GO) particles have lower conductivity compared to ethylene glycol/water, so as the concentration of graphene oxide (GO) particles increases, the number of particles with low conductivity also increases, reducing the solution's ability to conduct electric current. The presence of carbonyl groups in the GO structure also contributes to the decrease in conductivity. Carbonyl groups have acidic properties, which can interact with ethylene glycol/water, producing compounds with different electric charges. Causing inhibition of the flow of electric charge in the solution, thus reducing its conductivity. It is crucial to limit the concentration of graphene oxide in the solution and establish the desired conductivity in automotive cooling systems.

c. FTIR Measurement

FTIR measurement was conducted by immersing the material Al6061 in ethylene glycol/water with varying concentrations of graphene oxide for 7 days. FTIR analysis is shown in Figure 4.

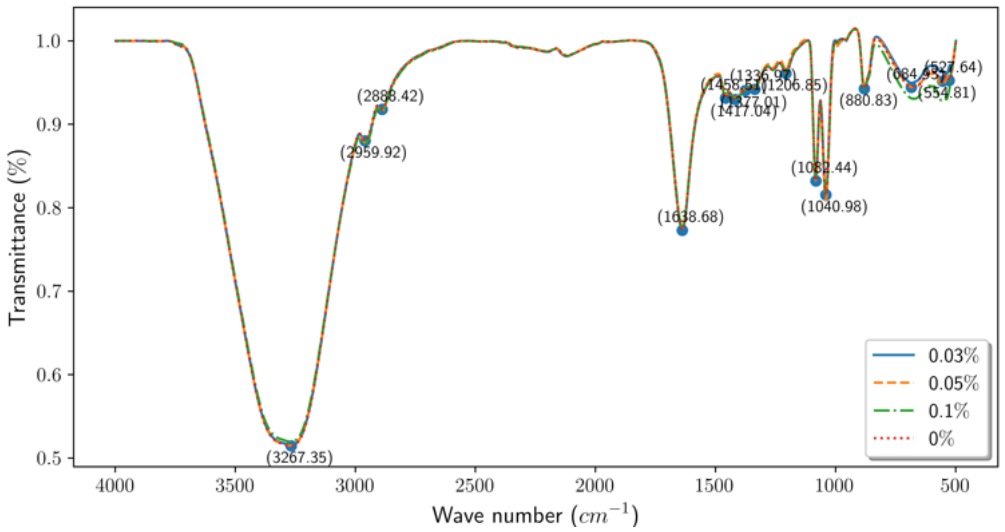

Figure .4. The absorbance spectra from the FTIR analysis.

The FTIR spectrum depicted in the figure displays several characteristic absorbance peaks, which are indicative of various functional groups present in the samples with different concentrations of graphene oxide (GO). The peak around 3267.35 cm^{-1} is typically assigned to the O-H stretching vibrations, suggesting hydroxyl groups, possibly due to moisture or hydroxyl functional groups on the GO. The sharp absorption at 2959.92 cm^{-1} and the peak at 2888.42 cm^{-1} can be attributed to the asymmetric and symmetric stretching vibrations of C-H bonds, indicating the presence of alkyl chains. Moving to the fingerprint region of the spectrum, the peaks at 1638.65 cm^{-1} and 1417.64 cm^{-1} could correspond to the C=C stretching vibrations from aromatic rings and the bending vibrations of C-H bonds in methylene groups, respectively. These peaks are characteristic of the graphitic structure of GO and its functionalized derivatives. The peak at 1040.98 cm^{-1} may be assigned to C-O stretching vibrations, commonly found on GO. The relatively consistent transmittance patterns across the different GO concentrations (0.03%, 0.05%, and 0.1%) suggest a uniform interaction of the functional groups with the ethylene glycol and water matrix. However, slight shifts and intensity changes in the peaks could indicate variations in the extent of interactions or the area of the functional groups due to changes in the GO concentration. The absorbance spectra from the FTIR analysis that can be drawn is that the formation of a protective layer on the surface of Al6061 material after the addition of Graphene Oxide (GO) in ethylene glycol/water solution.

d. Electrochemical Measurement

Potential polarization is a common test method used to determine the corrosion rate of a material. This method is based on the change in the electrical potential of a metal electrode when subjected to an electric current under dynamic conditions, where the electrode potential is gradually changed towards the anodic direction (more positive potential) or the cathodic direction (more negative potential). The potential polarization measurement obtains various electrochemical parameters such as Ecorr, βa, βc, and i_{corr}. The corrosion inhibition efficiency of corrosion inhibitors can be calculated from i_{corr} using equation 1. Corrosion rate analysis on Al6061 material was conducted with two treatments: variations in concentration in graphene oxide as a corrosion inhibitor in Ehylena glycol/water (W/EG, W/EG 0,03% GO, W/EG 0,05% GO dan W/EG 0,1% GO) and variations in ambient temperature (30 ºC, 40 ºC, and 50 ºC). The addition of GO as a corrosion inhibitor demonstrated a shift in the corrosion potential (E_{corr}) towards a more positive direction and a decrease in corrosion current density (i_{corr}), indicating a reduction in corrosion rate and higher

inhibition efficiency. This suggests GO's efficacy in forming a protective barrier on the Al6061 surface, which is further supported by the observed adsorption process. The influence of temperature on corrosion rates revealed that higher temperatures accelerate corrosion processes due to increased chemical reaction rates and ion mobility, underscoring the temperature-dependent nature of corrosion.

$$\eta\ (\%) = \left(\frac{i^0\ corr - i\ corr}{i^0\ corr}\right) x\ 100\ \% \qquad \text{Eq.1}$$

The electrochemical parameters obtained from Tafel polarization are presented in the figure. 5 and Table 3. In determining the corrosion rate, we use gamry software . There is a shift in the potential corrosion value (E_{corr}) towards a more positive direction compared to the blank solution (solution without inhibitor). The corrosion current density (i_{corr}) data generated by adding graphene oxide decreased compared to the blank current density value. This result indicates that the lower the current density value (i_{corr}), the lower the corrosion rate, and the higher the inhibition efficiency (η). This identifies the adsorption process of graphene oxide on the surface of Al6061 material. The adsorption process is indicated by the formation of a film layer as a physical barrier, protecting the Al6061 material from the corrosion process.

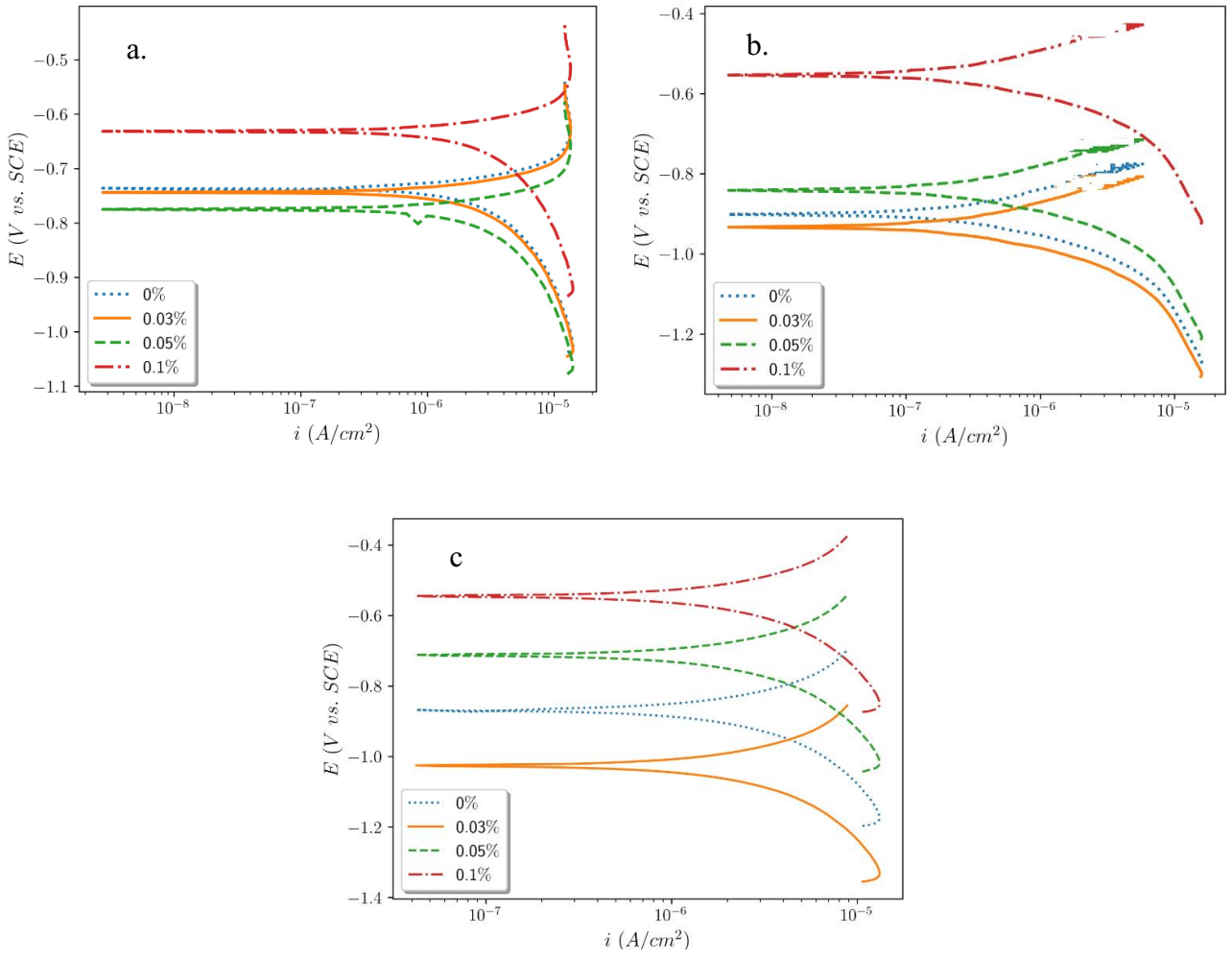

Figure. 5. Potentiodynamic polarization of Al 6061 in ethylene glycol/water with the absence and presence of graphene oxide at (a) 30 ºC, (b) 40 ºC, and (c) 50 ºC.

Figures 5 show that the potentiodynamic polarization curves of Al 6061 in ethylene glycol/water mixtures at varying temperatures show the impact of graphene oxide concentrations on the material's corrosion resistance. Notably, the addition of graphene oxide shifts the polarization curves towards lower current densities, indicating a decrease in corrosion rates, which is especially prominent at higher temperatures. At 30°C, the presence of graphene oxide shifts the corrosion potential (E_{corr}) to more negative values. It reduces the current density across all concentrations, suggesting that even at lower temperatures, graphene oxide contributes to a passive layer formation, enhancing the alloy's resistance to corrosion. Increasing the temperature to 40°C and 50°C leads to even more pronounced shifts in the E_{corr} and current densities, with the 0.05% concentration of graphene oxide showing a significant reduction in corrosion rate. This illustrates that the graphene oxide not only maintains its protective qualities at elevated temperatures but its efficacy as a corrosion inhibitor improves, likely due to better surface coverage or interaction with the metal surface. The reduction in corrosion rate with increased graphene oxide concentration suggests a potential for using graphene oxide as a protective agent in coolant systems where ethylene glycol is used, especially at higher operating temperatures where corrosion typically accelerates. The performance improvement at 0.05% concentration across the temperatures tested demonstrates the effectiveness of graphene oxide in enhancing the durability of Al 6061 in aggressive environments. The electrochemical parameters of Al6061 in graphene oxide-ethylene glycol/water, like shown in Table 3.

Table. 3. Electrochemical parameters of Al6061 in graphene oxide-ethylene glycol/water

T (ºC)	**Concentration Graphene Oxide**	**B_c** (V/decade)	**E_{corr} (mV)**	**i_{corr}** (A/cm²)	**CR (mpy)**	**Inhibition Efficiency (%)**
30 ºC	0	548,6x10^{-3}	-901,1	3,592x10^{-6}	4,620	
	0.03 %	514,7 x10^{-3}	-922,9	3,255 x10^{-6}	4,187	28.39
	0.05 %	404,4 x10^{-3}	-907,0	2,186 x10^{-6}	2,812	44,48
	0.10 %	268,6 x10^{-3}	-647,1	782,1 x10^{-6}	1,006	78,22
40 ºC	0	472,3 x10^{-3}	-867,4	3,550 x10^{-6}	4,728	
	0.03 %	432,6 x10^{-3}	-984,8	1,976 x10^{-6}	2,541	46,25
	0.05 %	369,8 x10^{-3}	-767,3	1,168 x10^{-6}	1,503	68,21
	0.10 %	234,0 x10^{-3}	-640,1	987,8 x10^{-6}	1,270	73,13
50 ºC	0	516,8 x10^{-3}	-735,9	4,377 x10^{-6}	5,629	-
	0.03 %	264,6 x10^{-3}	-769,7	8,908 x10^{-6}	3,146	44,11
	0.05 %	435,0 x10^{-3}	-788,6	2,292 x10^{-6}	2,947	47,64
	0.10 %	278,8e-3	-667,5	1,121e-6	1,441	74,40

The electrochemical parameters of Al6061 alloy in a graphene oxide-ethylene glycol/water mixture as shown in Table 3, provide insightful data into the corrosion behavior of this alloy at various temperatures and graphene oxide concentrations. At 30°C, a clear trend can be observed: increasing the concentration of graphene oxide decreases both the corrosion current density (i_{corr}) and corrosion rate (CR), while simultaneously increasing the inhibition efficiency. This trend indicates that graphene oxide acts as an effective corrosion inhibitor at 30°C, with the inhibition efficiency peaking at 0.05% concentration. As the temperature increases to 40°C and 50°C, the overall inhibition efficiency generally improves, highlighting the compound's capacity to protect the metal surface more effectively at elevated temperatures, which typically accelerate corrosion processes. At 40°C, the corrosion current density sees a substantial decrease with the introduction of 0.10% graphene oxide,

suggesting that this concentration creates an optimal barrier against the corrosive environment. At 50°C, the trend becomes slightly inconsistent; while the 0.03% concentration does not perform as well as the 0.05% concentration, the 0.10% concentration shows a decrease in effectiveness compared to the 0.05% concentration, as indicated by the higher corrosion rate and lower inhibition efficiency. This could imply that there is a critical concentration range where graphene oxide achieves maximum protection, and beyond this range, the effectiveness diminishes, possibly due to agglomeration effects or the instability of the graphene oxide dispersion at higher concentrations. The data also reveal that the corrosion potential (E_{corr}) becomes more negative with the addition of graphene oxide, particularly at 40°C and 50°C. This shift could signify the formation of a more stable passive layer on the Al6061 surface, further corroborating the protective nature of graphene oxide in the mixture.

Isotherm Adsorption Calculation

The Langmuir Adsorption Isotherm theory is used to identify the interaction between an inhibitor and the surface of Al6061. By utilizing Langmuir theory calculations, we can determine the type of adsorption phenomenon occurring on the Al6061 surface, whether it's physisorption or chemisorption. The calculation for the Langmuir adsorption isotherm equation 2.

$$\theta = \frac{IE\,\%}{100} \qquad \text{Eq.2}$$

It is to find θ (theta), followed by obtaining K_{ads} using equation 3.

$$K_{ads} = \frac{\theta}{c(1-\theta)} \qquad \text{Eq.3}$$

ΔGads (free energy of adsorption) is determined using equation 4.

$$\Delta G^o = -\,RT\ Ln\ (55 \times K_{ads}) \qquad \text{Eq.4}$$

The calculation results show the ΔG_{ads} values for the graphene oxide with each concentration addition as an inhibitor. The complete values of free energy of adsorption can be found in table 4.

Table 4. Free Energy of adsorption in graphene oxide on surface Al6061

Temperature	Concentration (%)	Efficiency	Surface Coverage (θ)	K_{ads}	ΔG_{ads} (kJ/mol)
30 °C	0	**0**	0	0	0
	0,03	28,39	0,2839	13,21510031	-16,597
	0,05	44,48	0,4448	16,02305476	-17,083
	0,1	78,22	0,7822	35,91368228	-19,116
40 °C	0		0	0	
	0,03	46,25	0,4625	28,68217054	-19,162
	0,05	68,21	0,6821	42,91286568	-20,210
	0,1	73,13	0,7313	27,21622627	-19,025
50 °C	0	0	0	0	
	0,03	44,11	0,4411	26,30762808	-19,542
	0,05	47,64	0,4764	18,19709702	-18,552
	0,1	74,4	0,744	29,0625	-19,809

The table shows the thermodynamic parameters for the adsorption of graphene oxide on Al6061 surfaces, with varying temperatures and concentrations providing key insights into the interaction dynamics. At 30°C, as the graphene oxide concentration increases from 0 to 0.1%, there is a notable enhancement in the inhibition efficiency, correlating with a concomitant rise in surface coverage (θ)

and adsorption constant (K_ads). This trend implies stronger and more extensive adsorption of graphene oxide on the Al6061 surface, as reflected by the increasingly negative free energy of adsorption (ΔG_ads), which intensifies from -16.597 kJ/mol at 0.03% to -19.116 kJ/mol at 0.1%. With the temperature increment to 40°C, a similar pattern is observed, with inhibition efficiency and surface coverage growing in tandem with graphene oxide concentration. The ΔG_ads values are consistently negative, signifying spontaneous adsorption. However, the adsorption is more favorable at this temperature, reaching -20.210 kJ/mol at a 0.05% concentration, suggesting that the interactions between graphene oxide and the Al6061 surface are possibly reinforced due to thermal effects. At 50°C, the inhibition efficiency sees a slight reduction at lower graphene oxide concentrations when compared to 40°C, but it improves markedly at a 0.1% concentration. This could be indicative of temperature influencing the adsorption behavior, where higher temperatures may require higher concentrations of graphene oxide to achieve similar coverage and inhibition efficiency as at lower temperatures. The surface coverage consistently increases with concentration across all temperatures, and the ΔG_ads values become more negative, suggesting that the adsorption of graphene oxide onto the Al6061 surface is inherently thermodynamically favored and becomes more stable with increasing concentration. Based on the value of ΔG_{ads}, the adsorption method on the Al6061 surface can be determined. According to Singh (2012), if the value of ΔGads is more positive than -20 kJ/mol, the formed adsorption process is physisorption. If ΔGads falls between -20 to -40, the adsorption process is a mixture of physisorption and chemisorption. On the other hand, chemisorption occurs when the value of ΔGads is more negative than -40 kJ/mol. In the corrosion inhibitor data generated, the ΔGads value is greater than -20 kJ/mol, indicating that the adsorption process between the Al6061 surface and the graphene oxide formed in this graphene oxide is a physisorption process.

4. Conclusion

Based on the data and analysis of the study it can be gathered that graphene oxide shows significant corrosion inhibition for Al 6061 in ethylene glycol/water solution. With increasing temperature and concentration of graphene oxide, there is an important increase in corrosion resistance, evidenced by a decrease in corrosion rate and an increase in inhibitory efficiency. Recommendation, it is necessary to optimize the concentration of graphene oxide to maximize protection at high temperatures without sacrificing solution stability. Further exploration may involve investigating the performance of graphene oxide in a wider range of temperatures and environmental conditions.

Authors' Declaration

We claim that all authors involved are major contributors

References

[1] R. Mohammad and R. Kandasamy, “Nanoparticle shapes on electric and magnetic force in water, ethylene glycol and engine oil based Cu, Al2O3 and SWCNTs,” *J. Mol. Liq.*, vol. 237, pp. 54–64, 2017, doi: 10.1016/j.molliq.2017.04.045.

[2] M. Krajčík and O. Šikula, “The possibilities and limitations of using radiant wall cooling in new and retrofitted existing buildings,” *Appl. Therm. Eng.*, vol. 164, no. October 2019, p. 114490, 2020, doi: 10.1016/j.applthermaleng.2019.114490.

[3] B. L. Jónsson, G. Ö. Gararsson, Ó. Pétursson, S. B. Hlynsson, and J. T. Foley, “Ultrasonic

Gasoline Evaporation Transducer - Reduction of Internal Combustion Engine Fuel Consumption using Axiomatic Design," *Procedia CIRP*, vol. 34, pp. 168–173, 2015, doi: 10.1016/j.procir.2015.07.061.

[4] H. Gürbüz, S. Demirtürk, İ. H. Akçay, and H. Akçay, "Effect of port injection of ethanol on engine performance, exhaust emissions and environmental factors in a dual-fuel diesel engine," *Energy Environ.*, vol. 32, no. 5, pp. 784–802, 2021, doi: 10.1177/0958305X20960701.

[5] B. Buonomo, L. Cirillo, O. Manca, and S. Nardini, "Effect of nanofluids on heat transfer enhancement in automotive cooling circuits," *AIP Conf. Proc.*, vol. 2191, no. December, 2019, doi: 10.1063/1.5138764.

[6] J. Kral, B. Konecny, J. Kral, K. Madac, G. Fedorko, and V. Molnar, "Degradation and chemical change of longlife oils following intensive use in automobile engines," *Meas. J. Int. Meas. Confed.*, vol. 50, no. 1, pp. 34–42, 2014, doi: 10.1016/j.measurement.2013.12.034.

[7] W. Yu, D. M. France, J. L. Routbort, and S. U. S. Choi, "Review and comparison of nanofluid thermal conductivity and heat transfer enhancements," *Heat Transf. Eng.*, vol. 29, no. 5, pp. 432–460, 2008, doi: 10.1080/01457630701850851.

[8] Y. Liang, S. Hu, J. Shen, H. Zhang, and P. Wang, "Journal of Materials Processing Technology Geometrical and microstructural characteristics of the TIG-CMT hybrid welding in 6061 aluminum alloy cladding," *J. Mater. Process. Tech.*, vol. 239, pp. 18–30, 2017, doi: 10.1016/j.jmatprotec.2016.08.005.

[9] R. Pourrajab, A. Noghrehabadi, E. Hajidavalloo, and M. Behbahani, "Investigation of thermal conductivity of a new hybrid nanofluids based on mesoporous silica modified with copper nanoparticles: Synthesis, characterization and experimental study," *J. Mol. Liq.*, vol. 300, p. 112337, 2020, doi: 10.1016/j.molliq.2019.112337.

[10] V. Sridhara and L. N. Satapathy, "Al 2 O 3 -based nanofluids : a review," pp. 1–16, 2011.

[11] I. Zakaria, W. H. Azmi, W. A. N. W. Mohamed, R. Mamat, and G. Najafi, "Experimental Investigation of Thermal Conductivity and Electrical Conductivity of Al2O3 Nanofluid in Water - Ethylene Glycol Mixture for Proton Exchange Membrane Fuel Cell Application," *Int. Commun. Heat Mass Transf.*, vol. 61, pp. 61–68, 2015, doi: 10.1016/j.icheatmasstransfer.2014.12.015.

[12] I. Zakaria, W. A. N. W. Mohamed, W. H. Azmi, A. M. I. Mamat, R. Mamat, and W. R. W. Daud, "Thermo-electrical performance of PEM fuel cell using Al2O3 nanofluids," *Int. J. Heat Mass Transf.*, vol. 119, pp. 460–471, 2018, doi: 10.1016/j.ijheatmasstransfer.2017.11.137.

[13] L. Li, X. Y. Liu, X. Wang, and M. Wu, "Effect of cooling methods on mechanical and corrosion properties of Inconel 625 during solution treatment," *J. Phys. Conf. Ser.*, vol. 1948, no. 1, 2021, doi: 10.1088/1742-6596/1948/1/012127.

[14] G. Kini *et al.*, "Corrosion in Liquid Cooling Systems with Water-Based Coolant - Part 1: Flow Loop Design for Reliability Tests," *Intersoc. Conf. Therm. Thermomechanical Phenom. Electron. Syst. ITHERM*, vol. 2020-July, no. Ml, pp. 422–428, 2020, doi: 10.1109/ITherm45881.2020.9190607.

[15] Q. Hu, Y. Liu, T. Zhang, and F. Wang, "Corrosion failure analysis on the copper alloy flange by experimental and numerical simulation," *Eng. Fail. Anal.*, vol. 109, p. 104276, 2020, doi: 10.1016/j.engfailanal.2019.104276.

[16] C. Y. Zheng, J. Y. Wu, X. Q. Zhai, G. Yang, and R. Z. Wang, "Experimental and modeling investigation of an ICE (internal combustion engine) based micro-cogeneration device considering overheat protection controls," *Energy*, vol. 101, pp. 447–461, 2016, doi: 10.1016/j.energy.2016.02.030.

[17] M. Sinha and R. K. Tyagi, "Strength and corrosion analysis in alloy steel and E-glass composite wear ring in automotive engine cooling water pump," *Mater. Today Proc.*, vol. 21, no. xxxx, pp. 1474–1478, 2020, doi: 10.1016/j.matpr.2019.11.054.

[18] N. Lebozec, N. Blandin, and D. Thierry, "Accelerated corrosion tests in the automotive industry: A comparison of the performance towards cosmetic corrosion," *Mater. Corros.*, vol. 59, no. 11, pp. 889–894, 2008, doi: 10.1002/maco.200804168.

[19] D. Özkan, Y. Erarslan, C. Kıncal, O. Gürlü, and M. B. Yağcı, "Wear and corrosion resistance enhancement of chromium surfaces through graphene oxide coating," *Surf. Coatings Technol.*, vol. 391, no. December 2019, p. 125595, 2020, doi 10.1016/j.surfcoat.2020.125595.

[20] N. Palaniappan, I. S. Cole, A. Kuznetsov, K. R. J. Thomas, B. K., and S. Manickam, "Experimental and DFT studies of gadolinium decorated graphene oxide materials for their redox properties and as a corrosion inhibition barrier layer on Mg AZ13 alloy in a 3.5% NaCl environment," *RSC Adv.*, vol. 11, no. 36, pp. 22095–22105, 2021, doi 10.1039/d1ra03495b.

[21] F. Zhang *et al.*, "The effect of functional graphene oxide nanoparticles on corrosion resistance of waterborne polyurethane," *Colloids Surfaces A Physicochem. Eng. Asp.*, vol. 591, no. December 2019, 2020, doi: 10.1016/j.colsurfa.2020.124565.

[22] H. Ijaz, H. Raza, G. A. Gohar, S. Ullah, A. Akhtar, and M. Imran, "Effect of graphene oxide doped nano coolant on temperature drop across the tube length and effectiveness of car radiator – A CFD study," *Therm. Sci. Eng. Prog.*, vol. 20, no. August, p. 100689, 2020, doi: 10.1016/j.tsep.2020.100689.

[23] R. Prasanna Shankara *et al.*, "An insight into the performance of radiator system using ethylene glycol-water based graphene oxide nanofluids," *Alexandria Eng. J.*, vol. 61, no. 7, pp. 5155–5167, 2022, doi: 10.1016/j.aej.2021.10.037.